Bello Hamza
ABDULLAHI

ENEHANCED QUANTUM EFFICIENCY OF PHOTOVOLTAIC SOLAR CELL BASED ON NANOPOROUS SILICON

M.S.
2014

# FATİH UNIVERSITY

**The Graduate School of Sciences and Engineering**

**Master of Science in**
**Electrical and Electronics Engineering**

## ENHANCED QUANTUM EFFICIENCY OF PHOTOVOLTAIC SOLAR CELL BASED ON NANOPOROUS SILICON

**by**

**Bello Hamza ABDULLAHİ**

**May 2014**

# ENHANCED QUANTUM EFFICIENCY OF PHOTOVOLTAIC SOLAR CELL BASED ON NANOPOROUS SILICON

by

Bello Hamza ABDULLAHI

A thesis submitted to

the Graduate School of Sciences and Engineering

of

Fatih University

in partial fulfillment of the requirements for the degree of

Master of Science

in

Electrical and Electronics Engineering

May 2014
Istanbul, Turkey

# APPROVAL PAGE

This is to certify that I have read this thesis written by Bello Hamza ABDULLAHI and that in my opinion it is fully adequate, in scope and quality, as a thesis for the degree of Master of Science in Electrical and Electronics Engineering.

_____
Assoc. Prof. Dr. Bayram ÜNAL
Thesis Supervisor

I certify that this thesis satisfies all the requirements as a thesis for the degree of Master of Science in Electrical and Electronics Engineering.

_____
Prof. Dr. Onur Toker
Head of Department

Examining Committee Members

Assoc. Prof. Dr. Bayram ÜNAL _____

Asist. Prof.Dr. Hüseyin SAĞKOL _____

Assoc. Prof. Dr. Abdülhadi BAYKAL _____

It is approved that this thesis has been written in compliance with the formatting rules laid down by the Graduate School of Sciences and Engineering.

_____
Assoc. Prof.Dr. Nurullah ARSLAN
Director

May, 2014

# ENHANCED QUANTUM EFFICIENCY OF PHOTOVOLTAIC SOLAR CELL BASED ON NANOPOROUS SILICON

Bello Hamza ABDULLAHI

M.Sc. Thesis – Electrical and Electronics Engineering
May 2014

Thesis Supervisor: Assoc. Prof. Dr. Bayram UNAL

## ABSTRACT

In this study, the quantum efficiency of silicon solar cells has been enhanced in some aspect. This is due to the limited electron/photon conversion in the existing solar cells. This was done by using anodization technique, and produced with the multilayered nanoporous on the surface with an average size of 5,9nm in diameter. These nano-porous surfaces were doped and form P-N junction. Moreover, the hetero-junction was formed between the crystal and nanoporous interface of the device which is important in the achievement of the aim. The doping method used is chemical method which involved one part of phosphorous tri-oxochloride to five part of acetone and was anealed at 800$^{O}$C under oxygen atmosphere. Finally, the two contacts were formed at front and backside of the device using gold and aluminum thin film, respectively. These contacts were formed as both ohmic and schottky junction. The efficiency was formed to be enhanced upto 22,06 %. While the efficiency of the standard silicon solar cells measured in our system is observed to be about 1,277 % for a comparison, the cells produced in our experiment showed an increase of the efficiency upto 20,788. Additionally, this type of the devices can be used as in the fabrication of LEDs and photodetectors, as in the case of photovoltaic applications.

**Keywords**: Optical Quantum efficiency, Porous Silicon, Heterojunction, P-N junction

# NANOGÖZENEKLİ SİLİSYUM TEMELLİ FOTOVOLTAİK GÜNEŞ PİLİNİN İYİLEŞTİRİLMİŞ KUANTUM VERİMLİLİĞİ

Bello Hamza ABDULLAHI

Yüksek Lisans Tezi – Elektrik-Elektronik Mühendisliği
Mayıs 2014

Tez Danışmanı: Doç. Dr. Bayram UNAL

## ÖZ

Bu çalışmada, silisyum güneş hücrelerinin kuantum verimliliği artırılmıştır. Bu, mevcut güneş hücrelerindeki sınırlı elektron / foton dönüşümünden kaynaklanmaktadır. Bu anotlama tekniği kullanılarak gerçekleştirilir ve çapı 5,9nm lik bir ortalama yüzeyi üzerinde çok katmanlı nanogözenekli üretildi. Bu nano-gözenekli yüzeyler katkılandırılmış ve PN eklemi oluşturulmuştur. Ayrıca, başarılı bir şekilde hetero-eklem, cihazların kristal ve nangözenekli arayüzeyinde arasında oluşturuldu. Kullanılan doping yöntemi, aseton beş kısmına fosfor tri-oxochloride bir bölümünü dahil edilen ve oksijen atmosferi altında, 800°C'de tavlanmış kimyasal bir yöntemdir. Son olarak, sırasıyla, altın ve alüminyum ince filmler kullanılarak, cihazın ön ve arka tarafında iki kontak oluşturuldu. Bu kontaklar, hem omik hemde Schottky eklemleri olarak oluşmuştur. Verimlilik 22,06 % 'e kadar geliştirmek üzere kuruldu. Karşılaştırmak için standard güneş pili hücresinin verimliliği yaklaşık olarak 1,277 % olarak ölçülürken, deneyimizde ki cihaz, % 20,788' e kadarlık bir artış sağlamaktadır. İlaveten, bu tür cihazlar, fotovoltaik uygulamalarda olduğu gibi, LED ve fotodetektör üretiminde de kullanılabilir.

**Anahtar Kelimeler:** Optik kuantum verimliliği, gözenekli silisyum, P-N eklemi

To my parents and the executive governor of kano state engineer (Dr) Rabiu Musa Kwankwaso

# ACKNOWLEDGEMENT

I gratefully thank my thesis supervisor Assoc.Prof. Dr. Bayram UNAL for his guidance and insight throughout the research. His suggestions and different viewpoints strongly helped me not only take a different approach to the research but also overcome the difficulties during the experimental part of thesis.

Thanks go to the other faculty members, Prof. Dr. Erkal İmal Prof. Dr.Onur Toker, and asst.prof. Hussein sagkol for their valuable suggestions and comments. The technical assistance of Bio and Nanotechnology Center, Asst. Prof.Dr. Yakup Bakıs, İsa seeker and Emre Göksel Yüzbaşıoğlu are gratefully acknowledged.

At last but not the least, I would like to thank TUBITAK for the scholarship awarded it is really encouraging.

# TABLE OF CONTENTS

# LIST OF TABLES

**TABLE**

# LIST OF FIGURES

**FIGURE**

# LIST OF SYMBOLS AND ABBREVIATIONS

**SYMBOL/ABBREVIATION**

| | |
|---|---|
| AC | Alternating Current |
| ARC | Antireflectio coating |
| CSLM | Confocal scanning laser optical microscope |
| DC | Direct current |
| DHF | Dilute Hydrochloric Acid |
| ECE | Electrochemical Etching |
| EQE | External Quantum Efficiency |
| HCL | Hydrochloric Acid |
| HF | Hydrofluric Acid |
| $H_2O$ | water |
| IBD | Ion Beam Deposition |
| IOM | Institute of Medicine |
| IQE | Internal Quantum Efficiency |
| $j_e$ | Current Density |
| LED | Light Emmiting Diode |
| LED | Light Emitting Diode |
| PECE | Photo-Electrochemical Etching |
| QE | Quantum efficiency |
| SC | Standard Clean |
| SEM | Scanning Electron Microscope |
| SEI | Scanning Electron Imaging |
| SOI | Silicon On Insulator |
| SPM | Sulfuric Peroxide |

# CHAPTER 1

# INTRODUCTION

In the Era of high technology and diversified electronics world, Electronics play a very important role in the human development through different aspect. Though a lot of challenges where faced by the engineers and researchers on how they can make the resources available, so that they make good use of them. Because of their scarcity, sometimes some alternatives have to be taken in order to provide those resources available.

For these reasons and more, make it necessary to study matter from its micro and nano level so that to alter some of its properties to suits the needs. All materials have difference in properties between its nano, micro and bulk state, Electronics components are the back bone of the entire circuits developed in the world, because all of them were developed from those components. Therefore, there is a need to make different studies in order to obtain such components using different method, different materials but with high efficiency.

Moreover, many efforts were made by different scientist surfer, concerning porous silicon, which is the main topic in these research, but in history porous silicon was discovered by a scientist called uhlir, accidently while performing electro-polishing experiments on silicon wafers using an electrolyte containing hydrofluoric acid. Its development was first justified for technological reasons, in particular, localized isolation in microelectronics. A renewed interest in porous silicon occurred in 1990 when its photoluminescence and electroluminescence properties were demonstrated. These doesn't stop at that, there are many more discoveries about such material across the world because of its importance especially in this field

Presently some of the mention devices are fabricated using high efficient materials like gallium arsenide example optical devices like light emitting diode (LED) and much more. Though silicon is cheaper than above mention gallium arsenide, but it can serve same purpose but only if its quantum efficiency is enhanced so that it provides enough photon to charge carrier ratio that can serve the aim. Now, this research will focus on enhancing quantum efficiency of silicon by improved the photon absorption of the material, because due to its refractive index(about 3.5) it reflect major part of the photon instead of absorbing and provides hole-electron pair which can serve our purpose. Most of the readers especially from fields other than engineering and science, may not understand some of the terms used surfer, therefore they are going to be elaborated and fully explain in the next few paragraphs.

Moreover, before then, let see some of the fields that require high efficiency of such silicon in order to obtain the device prescribed and role of porous silicon in each of those applications. The table below explains all of it.

## 1.1 QUANTUM EFFİCİENCY (QE)

The quantum efficiency (QE), of a photosensitive devices (i.e any device that produce charge when light falls on it) is the percentage of photons hitting the surface that produce charge carriers (i.e Photoluminescence). It is measured in electrons per photon or amps per watt. QE of a solar cell is a measurement of a charge carries produced by the solar cells when light excited on it. Since the energy of a photon is inversely proportional to its wavelength, QE is often measured over a range of different wavelengths to characterize it's efficiency at each photon energy level. The QE for photons with energy below the band gap is zero. Literally, band gap is the separation or distance between the top of the valence and bottom of the conduction bands. For an electron to transited from one band to another, it has to have an energy equals to at least the energy between the gap which is called band gap energy.

## 1.2 TYPES OF QUANTUM EFFİCİENCY

Two types of quantum efficiency of a solar cell are often considered:

**External Quantum Efficiency (EQE)** is the ratio of the number of charge carriers collected by the solar cell to the number of photons of a given energy *shining on the solar cell from outside* (incident photons).

**Internal Quantum Efficiency (IQE)** is the ratio of the number of charge carriers collected by the solar cell to the number of photons of a given energy that shine on the solar cell from outside *and* are absorbed by the cell.

In general the IQE is mostly larger than the EQE. A low IQE indicates that the active layer of the solar cell is unable to make good use of the photons. For the measurement of IQE, EQE of the solar device has to be measured first, then measures its transmission and reflection, and combines these data to infer the IQE.

$$EQE=\left(\frac{\frac{electrons}{sec}}{photons/sec}\right)=\left(\frac{current/(charge\ of\ 1\ electron)}{(total\ power\ of\ photons)/(energy\ of\ 1\ photon)}\right) \quad (1.1)$$

Table 1.1 Potential application areas of porous silicon [Adapted from 1].

| Application Area | Role of Porous silicon | Key Properties |
|---|---|---|
| Phtoelectronics | LED<br>Waveguide<br>Field emitter<br>Optical memory | Efficient electroluminescence<br>Tunability of refractive index<br>Hot carrier emission<br>Non-linear properties |
| Micro-optics | Fabry-Pérot Filters<br>Photonic bandgap structures<br>All optical switching | Refractive index modulation<br>Regular macropore array<br>Highly non-linear properties |
| Energy conversion | Antireflection coatings<br>Photo-electrochemical cells | Low refractive index<br>Photocorrosion cells |
| Environmental monitoring | Gas sensing | Ambient sensitive properties |
| Microelectronics | Micro-capacitor<br>Insulator layer<br>Low-k material | High specific surface area<br>High resistance<br>Electrical properties |
| Wafer technology | Buffer layer in heteroepitaxy<br>SOI wafers | Variable lattice parameter<br>High etching selectivity |
| Micromachining | Thick sacrificial layer | Highly controllable etching |
| Biotechnology | Tissue bonding<br>Biosensor | Tunablet chemical reactivity<br>Enzyme immobilization |

The external quantum efficiency therefore depends on the two phenomena absorption of light and the collection of charges. The photon is being absorbed and then generated an electron-hole pair, these charges are separated and collected at the junction. A "good" material avoids charge recombination which causes a drop in the external quantum efficiency. The ideal quantum efficiency graph has a square shape, where the QE value is fairly constant across the entire spectrum of wavelengths measured. However, due to the effects of recombination the QE for most solar cells is reduced, where charge carriers are not able to move into an external circuit. The same mechanisms that affect the collection probability also affect the QE. For example, modifying the front surface can affect carriers generated near the surface. And because high-energy (blue) light is absorbed very close to the surface, considerable recombination at the front surface will affect the "blue" portion of the QE. Similarly, lower energy (green) light is absorbed in the bulk of a solar cell, and a low diffusion length will affect the collection probability from the solar cell bulk, reducing the QE in the green portion of the spectrum. Generally, solar cells on the market today do not produce much electricity from ultraviolet and infrared light (<400 nm and >1100 nm wavelengths, respectively); this light is either filtered out or absorbed by the cell, heating the cell.

Therefore, these study will make the solar cells more efficient and reduced the loses from the effects discuss suffer. it’s very important to consider the cost, and the resources utilize during energy production, for that, to improve the quantum efficiency is a very important way to conserved resources as well as the effort toward this application.

## 1.3 ANTİREFLECTİON COATİNG (ARC)

Surfer we understood one of the effect that decreases the quantum efficiency of silicon, because of the refractive index between air and the silicon surface which

entirely reduces the absorption of the photons by the surface. Though different approaches were used by scientist, but the problem was the alternative method they took it either reduces the conductivity of the material or increases the resistivity which also alter the quantum efficiency. Therefore, by borrowing the technique that has been well developed in optical science, producing a porous on the silicon surface will reduce such reflection and serve as ARC.

Basically this technique uses Bragg reflection phenomenon, that is an interference effect caused by thin film structure. Figure-1 illustrates the process of Bragg reflection occurrence by the mirror stack structure. The reflectance occurs when the light incidence on an interface of two material with different index of refraction $n1 \neq n2$.[2]

The maximum reflection intensity occurs when the following condition is set and called as Bragg equation

$$n\lambda = 2\,d\,\sin\Theta \qquad (1.2)$$

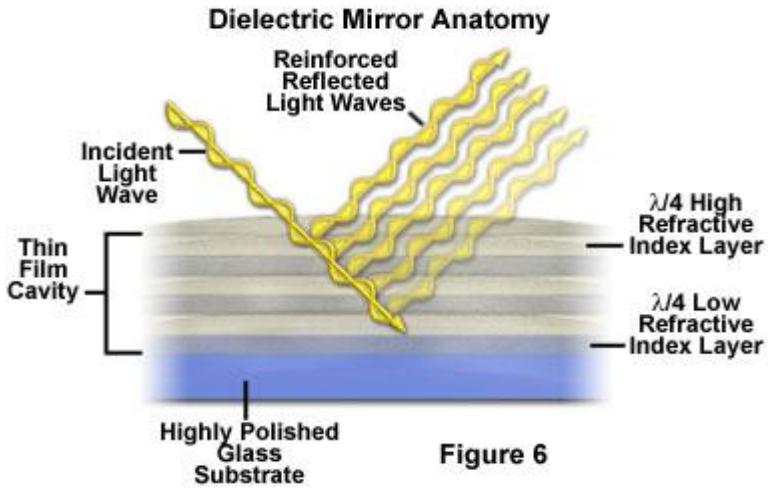


Figure. 1.1 Bragg reflection effect of mirror stacks structure with distance $d = \lambda/2$.(20)

For normal incidence $\theta = 90^{o}$, with Bragg equation, distance between mirrors needed for constructive interference reflectance is $d = \lambda/2$. While for the requirement of

destructive interference reflectance or constructive interference transmittance, the distance between mirrors is $d = \lambda/4$.

# CHAPTER 2

# LITERATURE REVIEW

## 2.1 INTRODUCTION

There are several methods used to etch silicon wafer/substrate to make it porous. These depend on the application in hand. Moreover, the properties of those wafers ranging from resistivity, orientation e.t.c all have an impact on the porous fabrication processes. Therefore we can simply describe silicon substrate as a high quality single crystals, nearly defect free, with a very low volume density of impurities and a controlled amount of dopants. The surface may also be flat on the atomic scale by some methods used in microelectronics. The formation of unidirectional pores on such ideal electrode materials is therefore intriguing since corrosion pitting is generally associated with material defects and leakage from a passive layer.

In this chapter, the literature review will be discuss by bringing all related literature to the topic and fully explain for good understanding of the whole topic. These will begins with anodization process been the backbone of porous silicon formation.

## 2.2 ANODİZATİON PROCESS

These process is an electrochemical process, which involve the passing of current through chemicals via the wafer in other to produces a porous across the current passage as well as the chemical which serve as the conductive as well as the etchant. Porous silicon (PS) is known to form during electrochemical dissolution of silicon in HF based solutions. This dissolution is obtained by monitoring either the anodic current or potential.

The anodisation cell is the double-tank cell where the wafer is in between the halve cells through which the two cells are connected electrochemically. This type of equipment (FIGURE 1) consists of two half-cells in which Pt electrodes are immersed and the silicon wafer is used to separate and isolate the two half-cells. HF is used for both anodisations of the polished side and as a back contact. A good uniformity is obtained by using symmetrical and large Pt plates as the cathode and the anode. The two Pt electrodes are connected to a power supply and the current flows from one half-cell to the other through the silicon wafer. The back-side of the Si wafer acts as a secondary cathode where the proton reduction takes place leading to hydrogen evolution. The front side of the wafer acts as a secondary anode where porous silicon is formed. [1]

…….

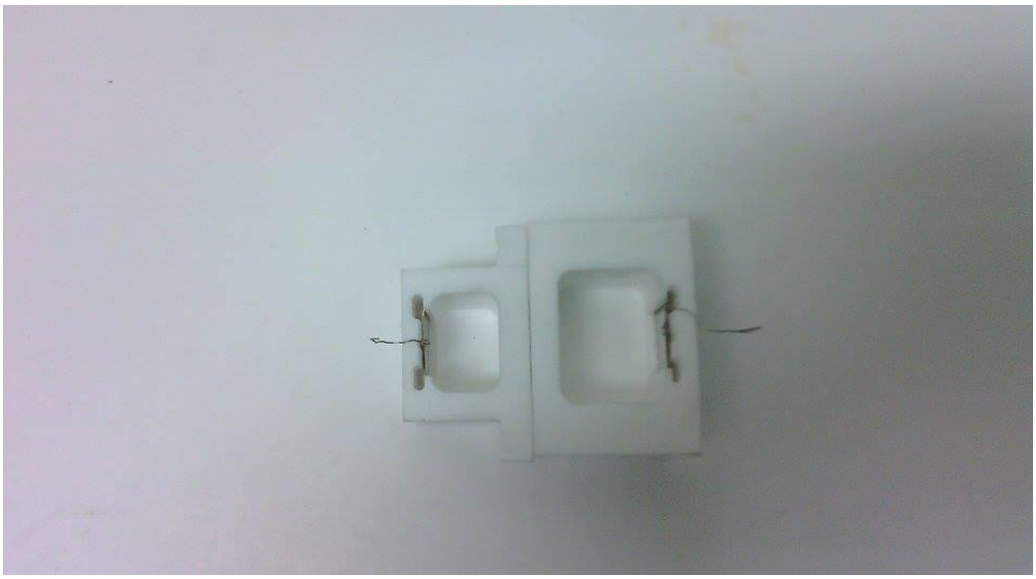

Figure 2.2 Top view of a 'double-tank cell'.

Further dissolution occurs only at the pore tips, where enough holes are available, as is schematically represented in Fig. 2. In this way the etching of porous silicon proceeds in depth with an overall directionality which follows the anodic current paths inside silicon. Once a porous silicon layer is formed no more electrochemical etching occurs but a slow chemical one starts, due to the permanence in HF.

For the case of n-type silicon, there is a need of back-side illumination by the application of light which allows further control on the hole injection. both in terms of carrier flux (which is proportional to illumination intensity) and of localization of the injection, which is concentrated in the region of the pore tips, acting as hole collectors. The etching process leads to a very regular pore growth, which is most effectively exploited to fabricate macro-porous photonic. Anodization process also depends on the wafer type. For p-type doped silicon, should be forward biasing during the process, while n-type doped silicon should be reverse biasing.

Furthermore, the current apply to these set up should be below critical current, which is the current at which the wafer can be damage if apply during anodization process.

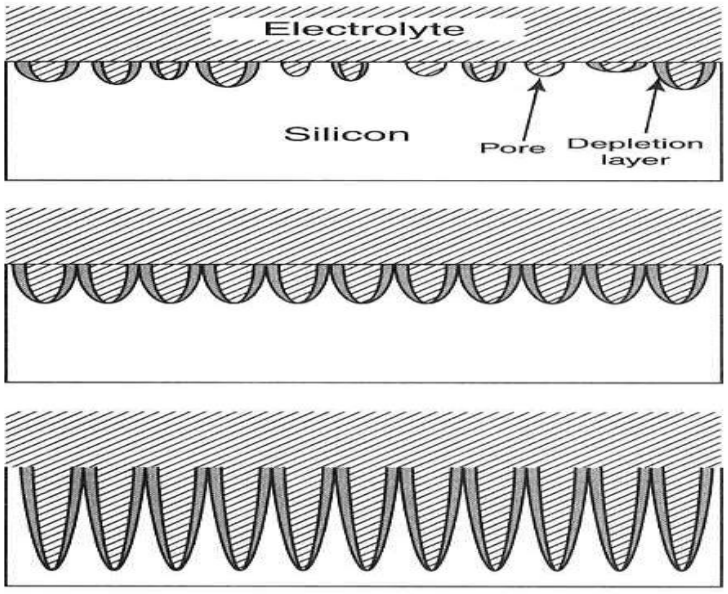


Figure. 2.3 Pore formation in porous silicon. The upper figure shows the initial stage, where the pores develop randomly on the silicon surface. In the middle, the self regulating process is shown. When the depletion zones around each pore overlap, the pore growth changes from an isotropic growth to a highly directional growth. The bottom figure shows how the dissolution advances only at the pore tips. (from 1)

Up to this point, we can say that the main requirements for porous silicon formation are:

1. The silicon wafer must be anodically biased. This corresponds to forward biasing for p-type doped silicon, and reverse biasing for n-type doped silicon.

2. For n-type doped and semi-insulating p-type doped silicon, light must be supplied.

3. Current densities below the critical value, *JPS*, must be used

The first two conditions are due to the fact that holes are consumed during the silicon etching. When the third condition is not fulfilled, the reaction is limited by mass transfer to the solution: holes pile up at the silicon-HF interface and electropolishing occurs.

For all the three conditions mentioned above the holes play an important role: in fact, porous silicon formation is a self-regulated mechanism, with hole depletion as the limiting agent. The dissolution reaction begins at defects on the silicon wafer surface, the pores are formed and their walls are eroded until they are emptied of the holes. This formation process protects them from further attack, and the reaction proceeds at the pore end, as is represented in Fig. 2.3.

The overall etching process is self-adjusting and the average pore size is given by the electrochemical parameters only. [2]

## 2.3 ANODİZATİON PARAMETERS

The porous silicon formation process using electrochemical (anodization) process, Involve some parameters that affect the process. These parameters can be use to determine as well as control the process. The parameters are:

The substrate doping.

The current density.

The HF concentration: the higher the concentration, the lower the pore size and the porosity. HF concentration determines *JPS* that is the upper limit to current density values. With a fixed and low HF concentration the range over which the current density can be varied is short, and it becomes wider by increasing the HF concentration.

The solvent where the HF is diluted: since porous silicon is organophilic and hydrophobic, the use of ethanol guarantees a higher homogeneity, due to a better wet-ability of the surface than de-ionized water.

The etching time: longer etching times lead to thicker layers, but for long time, anisotropy in depth in the layer due to the chemical action of the electrolyte is introduced.

The illumination during the etch, specifically for n-type substrates is needed. The porosity, thickness, pore diameter and microstructure of porous silicon depend on the anodization conditions are related, as is briefly describe in Table 2.1. These conditions include HF concentration, current density, wafer type and resistivity, anodization time, illumination (required for n-type silicon and semi-insulating p-type silicon), temperature, ambient humidity and drying conditions.

For a fixed current density, the porosity decreases when HF concentration increases. Fixing the HF concentration and the current density, the porosity increases with the thickness. This happens because of the extra chemical dissolution of the porous silicon layer in HF. [2]

The thickness of a porous silicon layer is determined by the time that the current density is applied, that is the anodization time. To have a thicker layer, a longer anodization time is required. For this reason, the periodic variation of the current density during the etching process allows the production of multi-layers formed by layers with different optical thicknesses.

Another advantage of the formation process of porous silicon is that once a porous layer has been formed, no more electrochemical etching occurs for it during the following current density variations. Hence, the porosity can be modulated in depth [3]. This fact allows the fabrication of any refractive index profile. A longer permanence time of silicon in HF solution results in a higher mass of chemically dissolved silicon. All these characteristics contribute to the easy formation of porous silicon, using double cell without the needs of expensive equipment only that the observations of porous properties involved expensive equipment.

Table 2.1 Effect of anodization parameters on porous silicon formation. An increase of the parameters of the first column leads to a variation of the elements in the rest of columns. (adopted from 2)

| | porosity | Etch rate | Critical current |
|---|---|---|---|
| HF concentration | Decrease | Decrease | Increase |
| Current density | Increase | Increase | - |
| Anodization time | Increase | Almost constant | - |
| Temperature | - | - | Increase |
| Wafer doping(P-type) | Decrease | Increase | Increase |
| Wafer doping(N-type) | increase | increase | - |

## 2.4 CONSEQUENCES OF POROUS SİLİCON DRYİNG

After the porous formation, desired structure will obtained, but if care is not taken the whole structure may be damage during drying, because it will crack and altered the original structured(i.e dimension of the porous formed). For example, If a 5 μm thick p+-type (0.01 Ω cm) PS layer of about 90% porosity is formed, it will gradually crack during drying. FIGURE l(a) exhibits the cracking, as revealed by scanning electron microscopy, of such a layer after the evaporation of water inside the pore network.

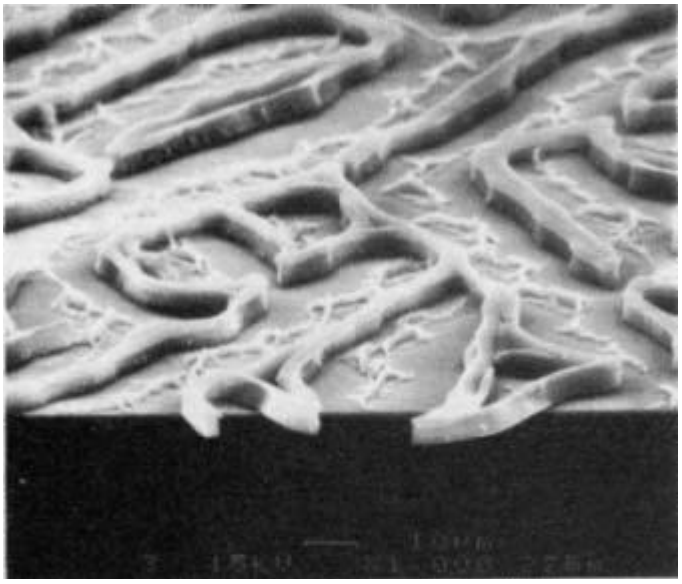

(a)

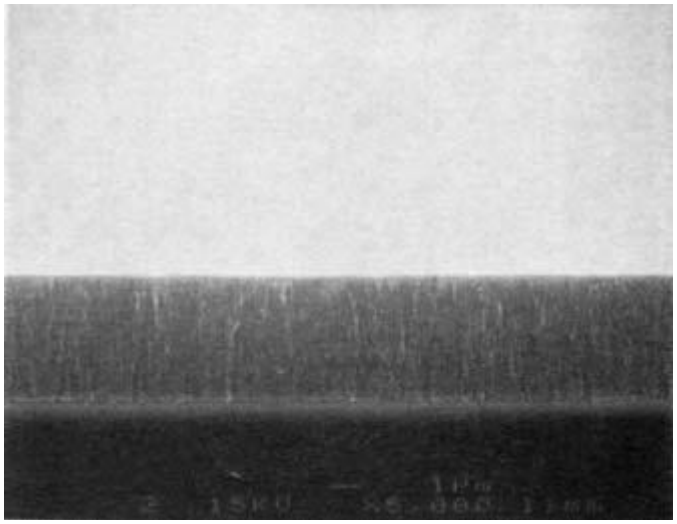

(b)

Figure 2.4 Scanning electron microscopy of a 5 μm-thick p-type porous silicon sample(of 90% porosity) after evaporation of: (a) water and (b) pentane.(adopted from 1)

It shows that crystalline perfection of porous silicon is altered during drying, which can be observed by X-ray diffraction.

Depending on applications, the required porosity can range from 20 up to 95%. For instance, silicon material with very low refractive index can easily be fabricated from highly porous silicon layer (used as a layer or in a multilayer). Moreover efficient photoluminescence of PS is observed on highly porous material (above 70%). Recently the optical properties of ultrahigh porous silicon films (prepared with supercritical drying) were investigated: by increasing porosity from 70 to 90%,the photoluminescence is considerably increased [1]. These examples, among others, show that highly PS films have interesting properties. However the use of highly porous silicon films has been limited by the mechanical instabilities during drying.

## 2.4 DRYİNG METHODS USED FOR POROUS SİLİCON

Different drying methods were proposed, these are shown briefly in table 2, with the basic features related to the studied samples and the results obtained. [1]

## 2.5 SUPERCRİTİCAL DRYİNG

Sur far, the efficient drying method is super critical drying, this method was first used by canham on porous silicon and then later others use same method. It involve the removal of the pore liquid which take place above the critical point, avoiding any interfacial tension. Ultra high porous luminescence structure result from this method which has porosity about 95% and is called aerocrystal.

## 2.6 FREEZE DRYİNG

For this method, the fluid inside the pore network is frozen and then sublimed under vacuum, then avoiding any interfacial tension. This was first trialed with small success by Gruning and Yelon [4] to dry p-type PS layers. In this method, the freeze drying allows only the drying stresses to be minimize and instead of a complete peeling

off the substrate (for normal air drying), a cracking pattern has observed [4]. Furthermore, after the first effort, the same technique has been more successfully applied by Amato et al [5], with trial on PS derived from p+1type substrates. In this effort PS layers was produced by anodisation of (111) silicon wafers and the porosity was above 70%. After the fabrication, the solution is frozen at -500C, followed by a sublimation under vacuum. For such PS samples, freeze drying was shown to be a non-destructive process, while air drying led to cracking. From this investigation [5], freeze drying appears to be simple to implement and is free of contaminating agents. The apparent disagreement between these two studies (i.e. [4] and [5]) could be related to the differences between the silicon substrates used or to some slight differences in the experimental conditions of the drying process. Clearly more studies are needed, since for instance it is well known that the thermodynamic behavior of confined fluid is different from that of bulk. Indeed, differential scanning calorimetric showed that the melting point of an organic fluid is lowered by a few tens of degrees when confined in the pore network of a PS layer [1].

## 2.7 DRYİNG WİTH PENTANE

The intensity and effects of the capillary stresses can also be reduced (but not eliminated) by using a drying liquid of lower surface tension than water. Pentane can be the right option for this purpose, because it has a low surface tension and in addition it observed that there is no chemical interaction with PS. Consequently, water and pentane are non-miscible liquids, we need an immediate liquid for them to interact, and ethanol can be used as an intermediate liquid. [1].

## 2.8 SLOW EVAPORATİON RATE

Pellegrini have developed a new drying method, by using a slow evaporation technique (after water or ethanol rinsing) on n+-type PS layers [1]. After sample fabrication, four different drying conditions have used to investigate their influence on

the optical properties of PS. It was then shown that a slow evaporation significantly improved the optical emission. [1].

## 2.9 P-N JUNCTİON

When P-type semiconductor make a contact with N-type semiconductor at the barrier of their contact they form what is called P-N junction. This junction is formed as a result of two current known as diffusion and drift current. At the contact there will be high concentration of the majority carries and low concentration of minority carries, as a result, due to the principal of diffusion in solids, majority carries diffused to either side of the junction for them to balance the concentration difference. This will not stop until they created electric field at the junction which as a result produce counter balance charge that will be opposite to diffusion current. This junction will form with both the charge carriers at the junction. This can be describe in the figure below:

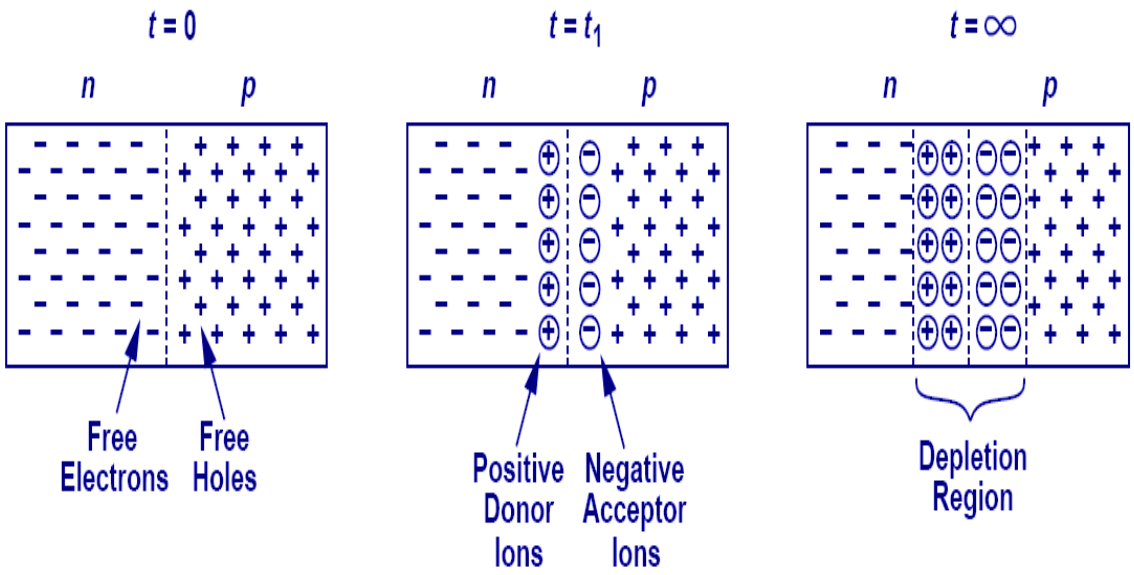


Figure 2.5 Formation of P-N junction (a) at t=0 beginning of the junction. (b) at t=t1 diffusion begin (c)at t=Ω P-N junction Formed

## 2.10 SPUTTER DEPOSİTİON

When an energetic particle strikes a surface (the target), a plume of material is released, like the shower of sand when a golf ball lands in the bunker. This effect is known as 'sputtering' and is used to produce films of materials as thin as just a few millionths of a millimeter. The source of the ions might either be a local plasma (diode or planar magnetron sputtering) or a separate ion beam source (ion beam deposition)[6].

## 2.11 PLANAR MAGNETRON SPUTTERİNG

If a strong magnetic field is applied the electrons follow a spiral path around the field lines giving them a much longer path length before being absorbed into a surface.

This greatly increases their chance of striking and ionizing an Argon atom and therefore gives the same ion density at a much lower pressure than for diode sputtering. If the

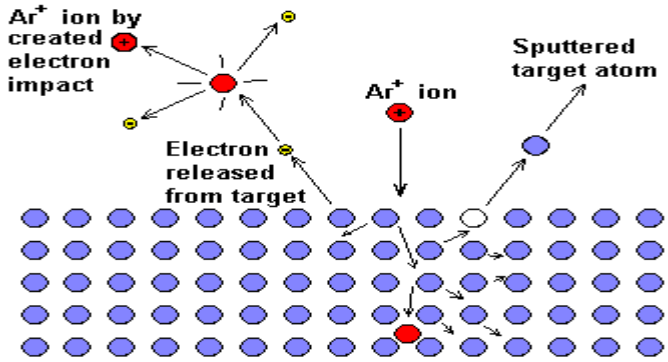


Figure 2.6 Sputter Deposition

ends of the magnetic field lines are at the cathode then the electrons will continue to bounce back and forward almost indefinitely. In planar magnetron sputtering a strong toroidal magnetic field confines the electrons in this way (leading to the distinctive toroidal plasma 'halo', right) and deposition at pressures as low as one millionth of an atmosphere. This allows for much higher deposition rates and more efficient usage of released material, but the toroidal plasma only erodes a 'race-track' in the target and little of the material near the centre or around the circumference can be used.

## 2.12 RF AND DC MAGNETRON SPUTTERİNG DEPOSİTİON.

When the Argon ion strikes the target an electron is released from the surface and combines with the ion to neutralize it, returning it to the vacuum as an Argon atom. If the target material is dielectric this process rapidly causes a charge build-up at the surface until Argon ions are no longer attracted, electrons are no longer released and the plasma extinguishes. To sputter non-conducting materials it is therefore necessary to apply AC or pulsed power to the target whereby the ion charge, which has built up on the surface, is expelled during the positive or neutral phase. Because the power supply is

only negative half the time, rates are lower than for DC sputtering whilst power supplies are more complex and therefore more expensive.

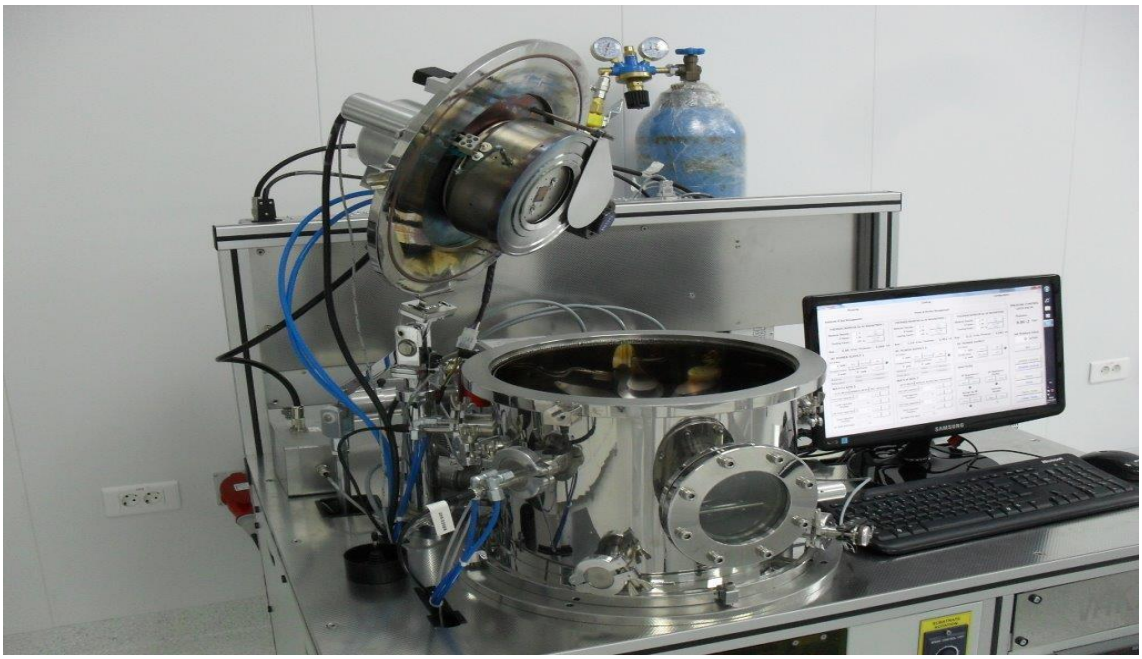

Figure 2.5 RF and dc Magnetron Sputter.

## 2.13 ION BEAM DEPOSİTİON

Alternatively, if the source of ions is not local to the target but is rather a neutralized beam, the electrical characteristics of the target are no longer of importance. In this technique, known as ion beam deposition (IBD) ions are extracted from a separate ion source to which the Argon is fed directly. The vacuum chamber pressure is therefore lower than that in the ion source allowing very low deposition pressures. IBD is often used in UHV systems and for ultra-clean applications. It also has the advantage that the energy with which the ions impact the target can be varied independently of other system characteristics such as ion density - both energy and rate can affect the characteristics of the film grown.

# CHAPTER 3

# METHODOLOGY

## 3.1 INTRODUCTİON

These steps involve the most important part of the whole project. The wafers used are N-type and P-type silicon of different orientation (111) N-type, (100) N-type and (100) P-type. All the three wafers mention are high resistive 1-5Ωcm², 1-5Ωcm² and 1-10Ωcm² respectively.

There are two condition involve, electrochemical etching (ECE) and photo-electrochemical etching (PECE) which involve the use of light. The average temperature in the room where the experiment took place was 20°C.

Initially, the wafers were prepared by cutting them in sizes that can fit in the double cell. Then the wafers were clean to remove any traces of dust, oil or finger print that may alter the resulting structure formed. The cleaning process used was standard RCA clean studied by Werner Kern which involve the following steps:

The RCA clean is known as a FEOL clean. The original RCA clean sequence is:

- Standard Clean 1 (SC1) - 5 volumes of H2O, 1 volume hydrogen peroxide (H2O2)
- 30%, 1 volume ammonium hydroxide (NH4OH) 29% was heated at 70 - 80oC.
- Ultrapure water rinsed.
- Standard Clean 2 (SC2) - 6 volumes H2O, 1 volume H2O2 30%, 1 volume
- Hydrochloric acid (HCl) 37% was heated at 70oC.Ultrapure water rinsed and dried.

- The SC1 clean takes out organic residues and particles. The SC1 clean works by creating and dissolving hydrous oxide films. The SC2 clean takes alkali metal and hydroxides - Li, Al, Ti, Zn, Cr, Fe, Ag, Pd, Au, S, Cu, Ni, Co, Pd, Mg, Nb, Te, W, Na, Fe (leaves Cl Residues)out.

The second method used is:

- Sulfuric Peroxide (SPM) - 4 volumes of sulfuric acid (H2SO4) 98%, 1 volume $H_2O$, 30% at 130oC for 10 to 15 minutes.
- Ultrapure water rinsed.
- Dilute hydrofluoric acid (DHF) 50 volumes H2O, 1 volume hydrofluoric acid (HF) 49% at room temperature for 10 seconds.
- Ultrapure water rinsed.
- SC1 for 20 minutes.
- Ultrapure water rinsed.
- SC2 for 15 minutes.
- Ultrapure water rinsed and dried.

The SPM makes the bulk organic removal and chemically oxidized the wafer surface in the anteceding sequence, the DHF removes the chemical oxide, SC1 removed particles and SC2 removed metals.

Furthermore, the silicon wafers dried using nitrogen gas before the etching process. The electrochemical process used is called anodization process. In this process the cell used is a double tank cell. So that the wafer was inserted in between the half cells. And the half cells where linked through a small circle through which the conduction take place from one half cell through the chemical via the wafer (i.e through the small circle that link the half cells) to the other half cell.

The area of the silicon that is within the circle was the etching site of the wafer, because is the only part that have a contact with the HF.

There are two platinum electrodes one in each of the half cell. This electrodes are used because they are HF resistance and conductive. The HF concentration can be obtained by considering the application in hand (i.e wafer properties).

The HF concentration is formed from the portion of the HF and surfactant in a certain proportions, in this thesis ethanol was used as surfactant with a percentage of 99.2% and the HF used is 40%. The concentration was selected from the suitable concentrations used by other literatures that wrote about solar applications using porous silicon. İn most of those literatures the concentration is 10%, but this concentration depend on the available chemicals in hand, because the concentration of the available chemicals determine the proportion. It can be calculated as follows:

To obtain a certain percentage we have;

$$\frac{axb}{a+c} = d\%$$

Where;

a= HF proportion used

b= HF concentration available

c=ethanol proportion needed

d= is the percentage concentration suitable fort he application in hand/

therefore, let take a=1, d=10%, and b=40% , to find c, we have:

$$\frac{1x40}{1+c} = 10$$

$$\rightarrow c = \frac{40-10}{10}$$

C= 3 portion

Therefore, the 10 % obtained comprises of 3 portion of ethanol 96% and 1 portion of HF 40%(i.e 3:1). This concentration is suitable for high resistive wafers, because the impurities are less, therefore the fluorine ion can reach the silicon easily and etch it away. But In contrary low resistive wafers have different case, since the impurities are are high, they can block the access to the silicon, therefore more HF concentration will be suitable for it.

## 3.2 ANODIZATION PROCESS

This experiment took place under fluorescent light at a temperature of 20°c with a double tank cell. This cell is an open cell without stirrer. Power supply is used to generate the current through the electrolyte, and to obtain the précised current density needed, and ammeter was used in series with the power supply so that the measurement is précised.

The cell is comprises of two separate chambers, where by stacked together by the used of bold and nut after placing the sample in between them. Certain precautions have taken before the beginning of the experiment, because it involves dangerous chemicals such as hydrofluoric acid. After the solution is prepared then the power generator is set to specification, the specification were:

The cell is filling up with the solution and then the platinum electrode were placed and crocodile jumpers are used to connect from the generator to the electrodes. Normally the negative terminal is placed on the face that the porous is willing to developed, and same is done here. The electric circuit is developed and current passed through the wafer via the solution in the adjacent cells. As a result, one face is etched and produced some porous layer. All the samples are fabricated the same way, though the result may vary, due to anodization parameters used, but in all cases the porous is formed as described.

There are nine samples obtained in all, three each from one type of silicon wafer mention in the beginning of this chapter. The samples prepared are as follows:

### 3.3 SİNGLE LAYER POROUS SİLİCON:

This was prepared with only single layer on the substrate (i.e same condition is used for the whole process). For this set of samples, the current density used is 20mA/cm² with solution concentration (i.e HF concentration) 10% at the duration of 20 minutes. In the case of N-type porous, illumination is needed, and this was done using a table lamp In all cases.

### 3.4 MULTİLAYERED ONE

This was prepared with double layered porous on the substrate (i.e different conditions were used for each layer). In the first layer, the current density is 50mA/cm² in a solution concentration of 10% at the duration of 10minutes, then suddenly the current was changed to 30mA/cm² but the remaining parameters remain the same until next 10 minutes. In all, the process take 20minutes from it starts.

### 3.5 MULTİLAYER TWO

This is also double layered porous, in the first layer, the current density used is 30mA/cm² in a solution of 10% at duration of 10minutes. The second layer has current density of 20mA/cm² with same condition as the first layer only the current density changes. In all the time duration was 20 minutes 10 for each layer.

## 3.6 DİSSOLUTİON CHEMİSTRİES

Yet, the accurate dissolution chemistries of Si in chemical solution are still not certain, but different approaches have been proposed. However, it is generally accepted that holes are required for both electro polishing and pores formation. During pore formation two hydrogen atoms evolve for every Si atom dissolved. The hydrogen evolution diminishes approaching the electro polishing regime and disappears during electro polishing. Current efficiencies are about two electrons per dissolved Si atom during pore formation, and about four electrons in the electro polishing regime. The global anodic semi reactions can be written during pore formation as

$$Si + 6HF \rightarrow H_2SiF_6 + H_2 + 2H^+ + 2e^-$$

and during electro polishing as

$$Si + 6HF \rightarrow H_2SiF_6 + 4H^+ + 4e^-$$

The final and stable product for Si in HF is in any case H2SiF6 or some of its ionized forms. This means that during pore formation only two of the four available Si electrons participate in an interfacial charge transfer, while the remaining two undergo corrosive hydrogen liberation. In contrast, during electro polishing, all four Si electrons are electrochemically active. Lehmann and Goessel have proposed a dissolution mechanism which is so far the most accepted. It is based on a surface bound oxidization scheme, with hole capture, and subsequent electron injection, which leads to the divalent Si oxidization state.

## 3.7 DRYING OF POROUS SILICON

The drying of porous silicon is done by a method explain below;

### 3.8 DRYİNG WİTH NİTROGEN GAS

The magnitude and effects of the capillary stresses has been reduced (but not eliminated) by the method used in the drying of the sample (i.e porous layer produced) , therefore nitrogen was used to dry the porous silicon so that the structure will not be damage by cracks.

### 3.9 DOPİNG

P-N junction is formed by doping N-type substrate at the porous site with P-type doping (i.e boron) likewise P-type substrate is doped with N-type at the porous site, hence the P-N junction is formed.

The method used in both cases to dope the impurities will be explained as follows;

### 3.10 DOPİNG N SUBSTRATE WİTH P İMPURİTİES

In this case, thin layer impurity is deposited on the porous site using sputtering in which a little portion penetrate through the nano wires porous while some remain at the surface. Later they are diffused to the silicon by annealing at a temperature of 900°C. This temperature is used knowing the melting temperature of silicon which is 1400°C, therefore it will not melt and it will be suitable for the purpose.

### 3.11 DOPİNG P SUBSTRATE WİTH N İMPURİTİES

This was done using chemical method. It involve combining one portion of POCL3 to five portion of acetone, then the solution is doped in the porous site and penetrate through the pores then dry, for uniformity, the solution is drop on the porous while its spinning on spinner. It was also annealed at 700°C using furnace.

### 3.12 RF AND DC MAGNETRON SPUTTERİNG DEPOSİTİON.

Aluminium film was deposited using this method. Ar+ Ions formed in a plasma are accelerated towards a target material(i.e Aluminium target). These high energy ions eject some amount of target material atoms. Then these atoms were transported to the substrate in vacuum. Since target atoms were not evaporated there is no need for high temperatures hence there are no hot parts in a sputtering system. Materials that cannot be deposited in an evaporator due to their high melting point can easily be deposited in a sputtering system.

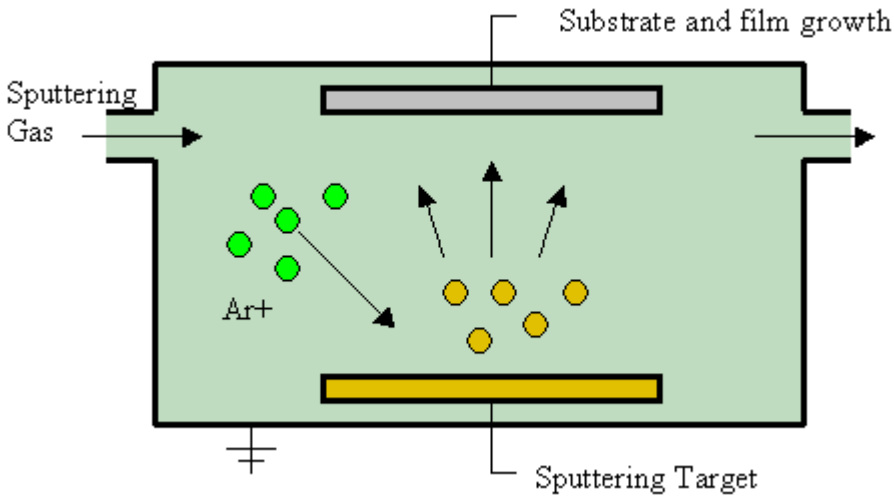


Figure 3.1 Description of RF and dc Magnetron Sputtering Deposition

### 3.13 ELECTRON BEAM DEPOSİTİON

The deposition of Gold film was carried out using this method. In this system, the target material is bombarded by a high energy electron beam. The arising heat energy evaporates the target material. The vapor from target material deposits on the substrate. By this technique, single crystal films at relevant growth conditions, amorphous thin films and many other structures can be growth on the substrate surfaces in a varying

thickness and dimension from nanometer to micrometer scale. But in this case the gold film was deposited using this method

# CHAPTER 4

# TECHNIQUES OF EXPERIMETAL MEASUREMENTS

## 4.1 INTRODUCTİON

In this chapter, the measurements obtained from the fabricated samples will be discussed. Since the fabrication is done, then we need to measure the results to see which effect we got because of the methods applied to the samples.

Before we start discussing the result, we need to explain briefly how the contacts where taking before the measurements. These has a significant effects on the result, because bad contacts may give falls results even if all the steps were right.

After the methods described in the third chapter, a copper wire of approximately 0.2mm in radius was use along with a silver paste to take the contact from both side of the wafer. The Picture of the sample is shown in figure 4.1.

As shown in figure 4.1, three contacts were taken. At the porous point one contact is taken as the positive potential, an at same porous side but the crystalline part another contact was taken, then the last contact from the back side of the sample.

## 4.3 CONFOCAL MİCROSCOPE (CSLM)

Confocal scanning laser optical microscopy (CSLM) is very important for luminescent studies. Based on the Luminescence, confocal microscopy can be explain as an emission of photons of lower wavelength generated by hitting sample atoms by an

incoming wave. To see the difference between confocal and widefield microscope, let us look at the working principle of these two microscopes. In a

tradionalwidefield microscope, all sample is illuminated simultaneously, on the other hand confocal

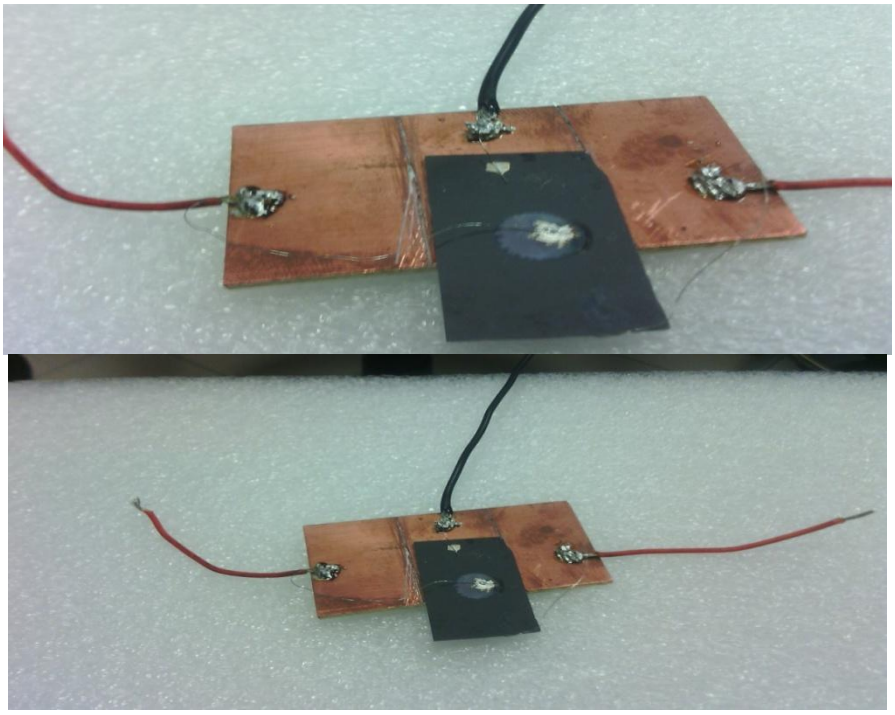

Figure 4.1 Picture of the sample produced with  the contacts.

microscope, a beam laser light is scanned in the small part of the sample. This occurs by formation point by point image. The structure of confocal microscope is given in figure 4.5. The most important part for the resolution of the image taken from confocal microscope is pinhole which blocks incoming light from out of focus. Therefore reject out of plane unfocused light to obtain a sharper, better resolved image. The optimum resolution is obtained by a tunable pinhole. In contrary, dichroic mirror is used to reflect light shorter than a particular wavelength but transmits light of longer wavelength. Thus, the light from the main source is reflected and sent through the objective to the sample, while the longer-wavelength light from the fluorescing specimen is sent through both the objective and the dichroic mirror. Furthermore, it is possible to construct 3 D shape of a volume of the specimen by collecting the data of a series of thin slices taken along vertical axis, it is z axis in this study [98]. For this, the detector is connected to a computer which forms the image one pixel at a time. For instance, a 512pixel x 512

pixel image is typically achieved at a frame rate of 0.1 to 30 Hz. In a study, the main two advantage of confocal microscope is written down below as:

Instead of at different angles as in the case of the scanning mirror configuration the specimen is everywhere exposed with ligth axially, therefore avoiding optical aberrations. Thus, the uniform illumination of the entire field of view is possible.

by handling the amplitude of the stage movements like increasing, the field of view can be augmented more than that of the static objective.

Figure 4.3 structure of confocal microscope, photo taken from Bio and Nano research center.

## 4.4 SEMİCONDUCTOR CHARACTERİZATİON SYSTEM

Model 4200-scs Semiconductor characterization system is an instrument use to test or measure several wafers characteristics. It perform this function by either sourcing current and measure voltage or sourcing voltage and measure current, from this result several characteristics can be obtained.

For an application that involves small area, this device interfaces and control another instrument known as probe station. In this mode the system initializes the prober driver and establish the reference site(die), and then instruct the prober to move the probe station chucks up or down making or breaking contact between the wafer and test system pins(probe needles), as such it test the required property.

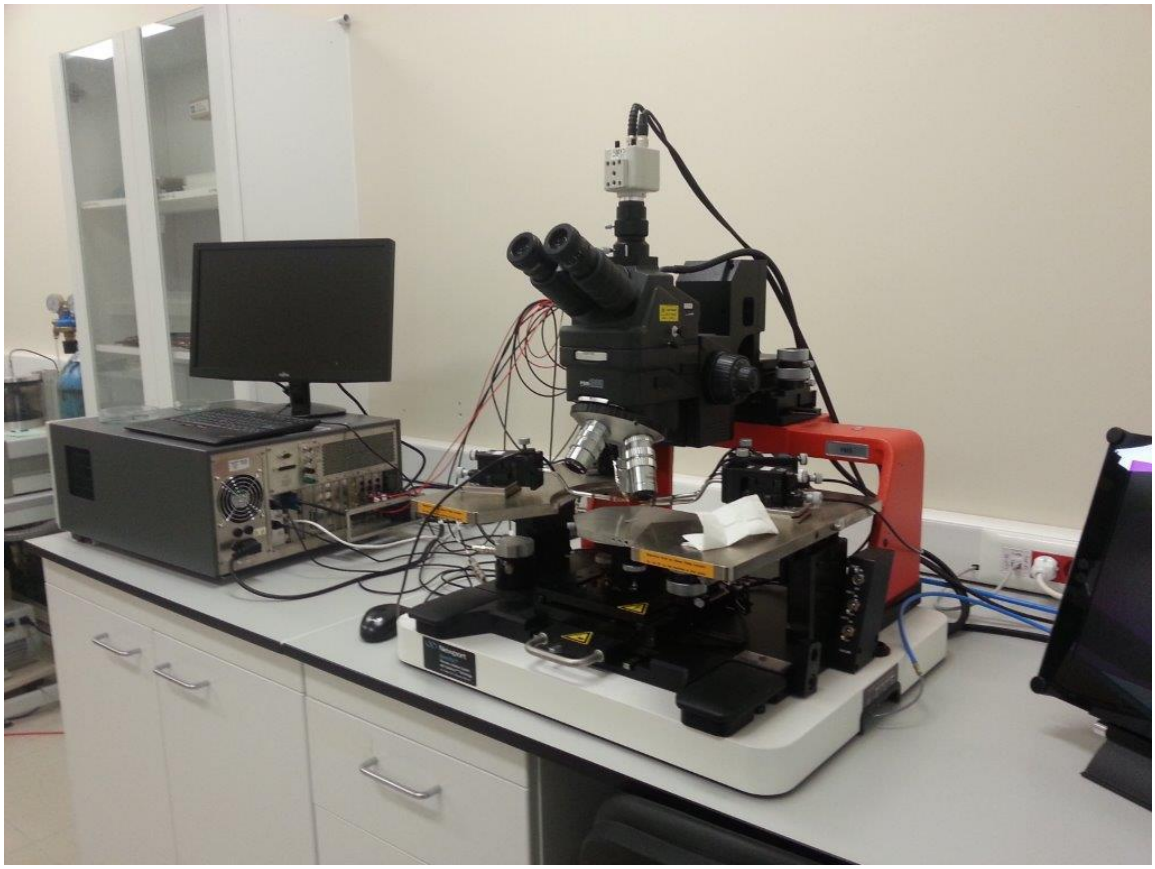

Figure. 4.4 semiconductor characterization system

## 4.5 SCANNING ELECTRON MICROSCOPE

Scanning Electron Microscope (SEM) is an instrument applied to conductive and sometimes nonconductive nanostructured samples at few until high kV and higher beam current. It is used for analytical applications requiring high resolution. SEM is employed to observe the surface structures by secondary electron images (SEI) and compositional distribution by backscattered electron images (BEI); it generate high resolution images of object. These was used to take the images of the samples shown in chapter five and observed the shapes of the pores so that to obtain some properties of suc pores in photovoltaic application.

Figure 4.5 Scanning Electron microscope.

## 4.6 CURRENT-VOLTAGE MEASUREMENT OF A SOLAR CELL

The instruments involves are:

I. solar cell module
II. ammeter

III. voltmeter
IV. variable resistor
V. alligator clips and jumpers
VI. Light source

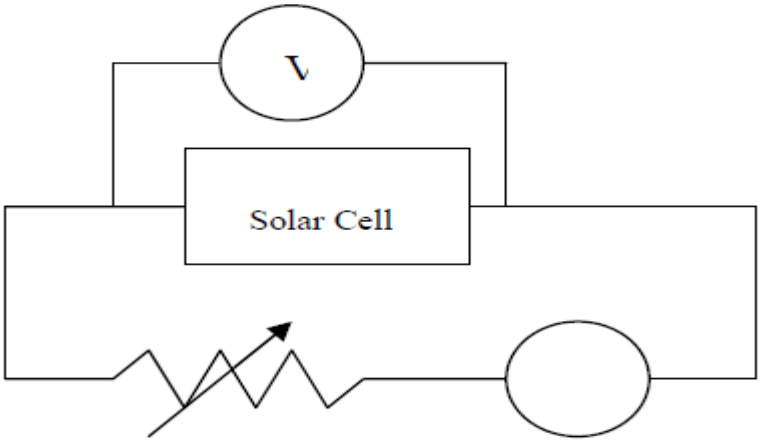


Figure 4.6 the set up for I-V measurement of a solar cell.

The circuit was set up as shown in figure 2.12, then the following methods were used to obtain the result;

Methods;

1. the circuit is in the diagram above ( Ammeter is in series, Voltmeter parallel)
2. the solar cell was set to faced towards a source of artificial light.
3. the Short Circuit Current was Measure ( by having maximum resistance) and Open Circuit Voltage (by disconnecting the variable resistor)
4. the resistance of the variable resistor was then Changed. Record the new current and voltage.
5. When the rate of changes of voltage has increased, should decrease the change in current and the. the current and voltage was measured and Recorded .
6. this was Continue until the maximum resistance in the variable resistor (when voltage = 0)

7. the data was Placed in MS. Excel. the IV curve was Plot, with current in the vertical axis, and voltage in the horizontal axis as seen in figure 5.2.
8. The current and voltage of each data set is then multiplied together giving a value for power and placed in the adjacent column.
9. another graph was plot, with power in the vertical axis, and the voltage in the horizontal axis. This is the power graph.
10. Indicate the maximum power in the power curve, and the respective voltage and current was found.

# CHAPTER 5

# DISCUSSION

## 5.1 INTRODUCTION

So far, we discuss about the topic and the expected result to achieve. After going various processes in the previous chapters by considering fast literatures, we developed more steps to the existing ones accordingly to improve the quantum efficiency positively. Now in this chapter, we can see the results tested from the samples prepared.

All the samples were prepared using same methods (anodization method) but different parameters, but they have same effect toward the efficiency. Therefore, the sample with the highest output shall be use to compare against the non etched silicon wafer from which the sample was prepare and see how much the efficiency is improve. In addition to that, we can take some of the measurement against standard existing solar cells and see which effect can be observe from the fabricated one.

The set of samples use in the thesis are P (100) high resistive with resistivity of 10ΩCm, N(100) high resistive and N(111) high resistive with the resistivity of 1ΩCm. in all cases three different set of samples were prepared single layer porous using anodization process with the current density of 20mA/cm², solution concentration(HF:ethanol) 10% and anodization time 20 minutes. These specifications have used for all the three samples to obtained single layered porous for each of the samples. The second sample is multilayered porous using same method but with the specifications current density one ( $j_i$) 50mA/cm², current density two ($j_2$) 30 mA/cm², solution concentration (HF:ethanol) is 10% and the times are 20 minutes for each layer. Same as in the first case these conditions are used for all the three samples. Then the last

set of samples were prepared using the same method but different specifications, this is also multilayer with current density one ( $j_i$) 30mA/ cm², current density two ($j_2$) 2mA/cm², solution concentration (HF:ethanol) is 10% and the times are 20 minutes for each layer.

Until now nine samples were prepared three set per each specification, all the specifications were obtain from the past literatures that study on solar cells efficiency, the optimized values where used so that to observed the effect on the efficiency of the Prepared sample. The SEM image obtained for the samples is shown in figure 5.1.

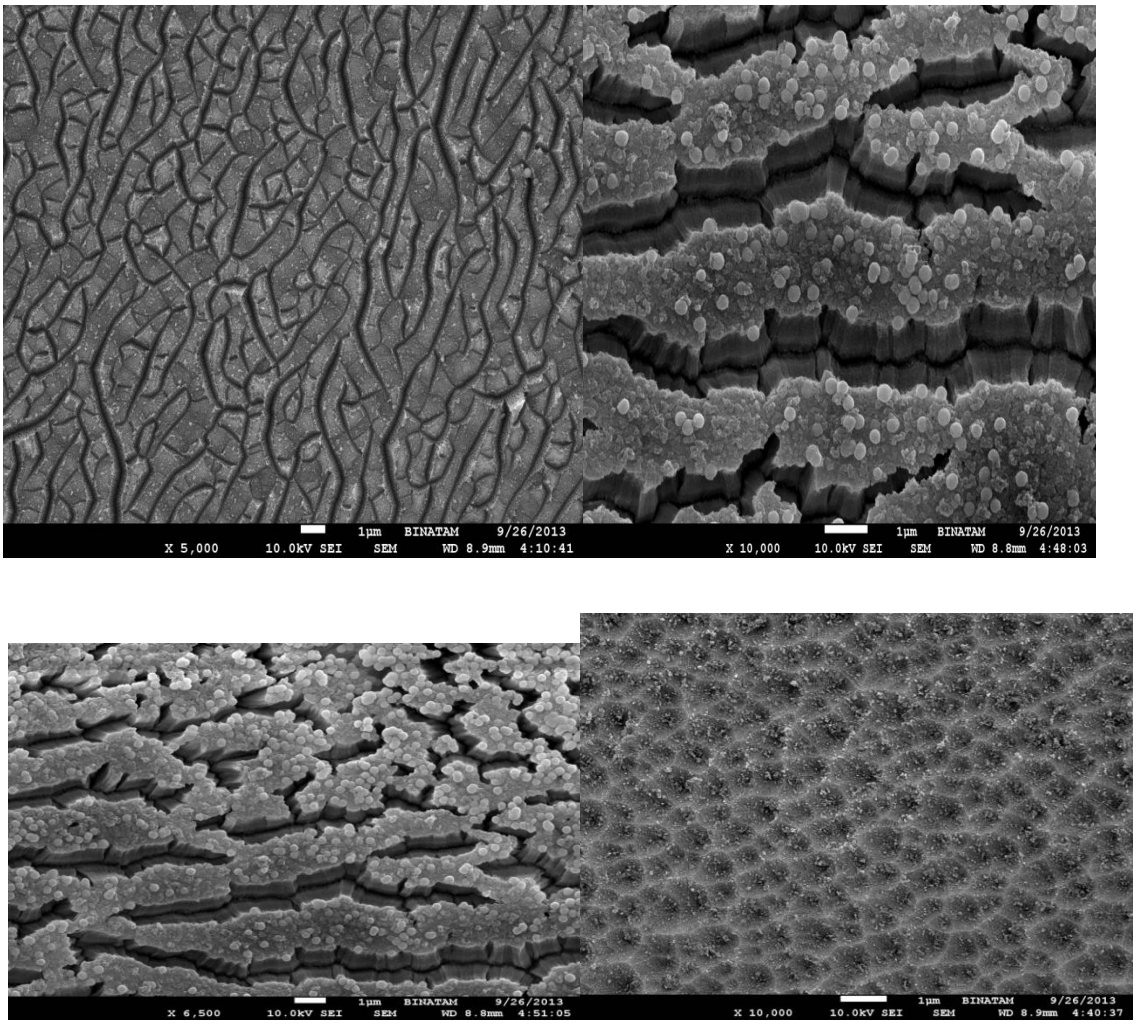


Figure 5.1 SEM images of the porous samples

As shown in fig 4.1, the surface of the c-Si sample was completely etched and consisted of numerous tiny pores formed over the soft wall. The formation of numerous new tiny pores inside the initial pores can be distinguished clearly. These pores results from the conditions used in the fabrication, double pores for multilayer and single pore for the single layer is clearly observed in the SEM image.

The approximate pore size obtained is in the range of few Nano-meters scale, these range is the suitable range for solar cells. There are highly dense pores on the surface which is also important for manipulating the surface to obtain the suitable way of improving absorption on the surface.

The porosity is high up to around 90% obtained from the following formula given in the literature;

$$P(\%)= \frac{m^1 - m^2}{m^1 - m^3} \qquad (5.1)$$

Where m1 is the sample weight before anodization, m2 is the sample weight after anodization, and m3 is the sample weight after removing the PS layer with 5% KOH solution for 60 s.

Fig. 5.1 illustrates the SEM image of the PS layer formed on the n-type c-Si (111) sample. The surface of the c-Si sample cracked, and pores were not evidently observed. The etched surface became rougher than the c-Si surface, indicating low porosity (approximately 14.5%).

Fig. 5.1 demonstrates the SEM image of the PS layer formed on the p-type c-Si (100) sample. Pores with sphere-like appearances and thick walls were evidently randomly distributed on the PS surface. A modest density of pores was observed, and porosity was approximately 45%, higher than the 27% porosity of the PS layer formed on the N-type c-Si (100) sample (Fig. 5.1). The surface of the c-Si sample cracked, and numerous new pores evidently formed inside the cracks. Additionally, the surface of the c-Si sample was completely etched and consisted of numerous discrete pores that

formed over the wall that did not crack, and the pore walls widened, reducing the number of pores on the PS surface. Hence, porosity decreased.

The average pore diameter (d) for the PS layer formed on the n-type c-Si (100) wafers was 5.9 nm and calculated using Eq. (2) below [18],

$$E(eV) = Eg + \frac{h^2}{8d^2}\left(\frac{1}{me^*} + \frac{1}{mh^*}\right) \quad (5.2)$$

where E (eV) is the energy band gap of the PS layer calculated from the PL peak. $E_g$ is the energy band gap of bulk c-Si. h is Planck's constant=$4.13\times10^{-15}$ eV·s, whereas M*e and M*h are the electron and hole effective masses, respectively (at 300 K, =$0.19m_o$, =$0.16m_o$, and $m_o$=$9.109x10^{-31}$ kg).

In single layered porous, only one layer with approximately equal porous distribution will be observed and the porosity of the layer depends on the solution concentration, current density, etching time and the doping of the substrate. Therefore low solution concentration (i.e 10%), high current density (i.e 20mA/cm²), longer anodization time (i.e 20minutes) and low doped wafer were used and high porosity is observed which is suitable for solar application.

For the multilayer porous, more porosity was observed do to the parameters used which favours high porosity since it has double layer each with suitable values for high porosity in the anodization process.

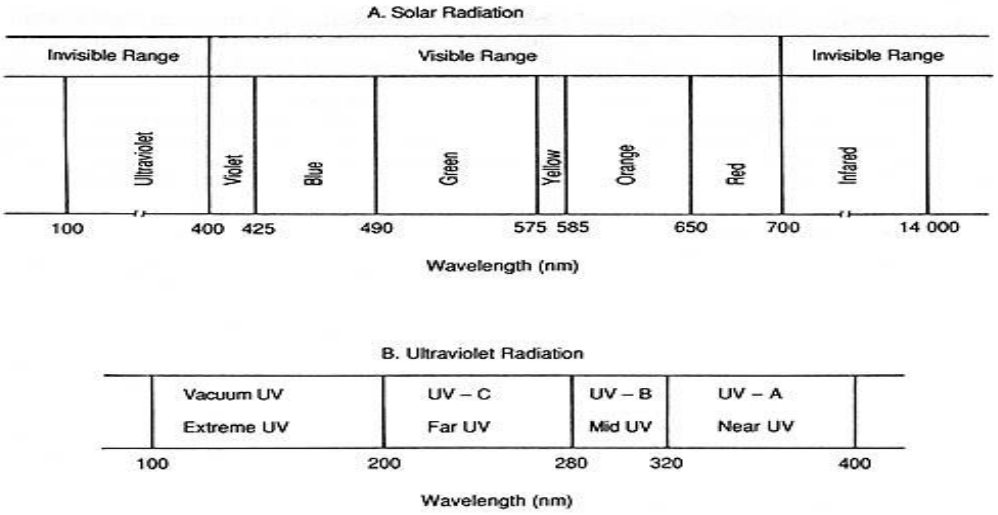


Figure 5.2 Solar spectrum

Fig 5.2 shows the solar spectrum with the wavelength of the solar radiation ranging from uv until infrared. The photovoltaic measurement (i.e microvolt against wavelength) done on the sample, it shows that there is an increase in the uv range compared to existing solar panel measured under same condition. The measurement start from 200nm until 1500nm from which we observed shift on the prepared sample which start producing voltage from 200nm while standard solar start from 300nm as seen in the fig 5.3.

Furthermore, there is an increase in the infrared region where the prepared samples end at 1500nm while standard solar ends at 1100nm. This results due to the hetero-junction existed between the crystal and the porous part of the silicon. This because of the change in the Fermi energy. Since Fermi energy level tries to be at a point where the charge carries are equal both at valance and conduction band in a semiconductor. The area where the silicon is etched, there will be a changed in the concentration of the charge carries, so the Fermi energy change in that particular position, but in the crystal part of the sample it remain where it is originally. The two Fermi energy of the porous and non porous site tries to align themselves, but due to different in level the Fermi energy bends and more charge carries gather on that point which created a voltage at that position.

In general, for the whole spectrum the prepared sample produces high voltage compared to existing solar as we can see in the fig 5.3 . This is due to the accumulated charges on the porous side, since it's doped with different impurity (i.e N-impurity for p-substrate and vice versa), due to that a p-n junction is formed which consist of charges accumulated at the junction barrier. And as well the hetero-junction I have explain surfer, due to this two junctions the voltage will be higher compared to the other part of the substrate, therefore the voltages observed per each spectrum is higher in the sample than the standard solar due to this reason.

Moreover, all the samples were mesured and the specturm is shown clearly that there is absorption from UV until infrared which shows that all the mmethods us are positively effective towards the efficiency of the sample (i.e crystalline silicon). Fig 5.4 shows these clearly.

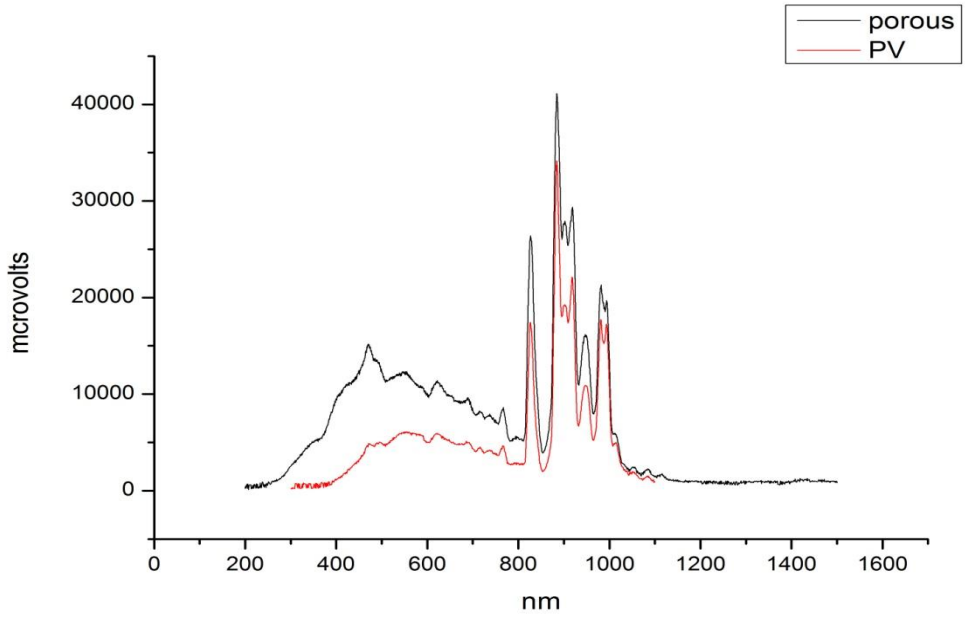


Figure 5.3 photovoltaic measurement of standard solar (i.e red C) and fabricated solar (i.e black B)

Furthermore, from fig 51, also we can see that almost all the spectrum is absorbed through the surface. Thi was due to anti reflection coating (ARC) of the porous layer.

Because now is a rough surface as a result of the etching, these layer it plays a vital role in the enhancement of quantum efficiency of a solar cell (i.e photo-conversion). These also increase the absorption in the visible region of the spectrum which is expected to increase the efficiency of the solar cells.

The I-V measurement was done using the method discuss in chapter four (i.e 4.6), the corresponding current and voltages were recorded then later the power is obtained. Using this results, the curve was plot I-V curve and power curve were all plot on same graph as seen in figure 5.4, the result are tabulated in table 4.1 as shown.

As shown in fig 5.4, the I-V curve of the sample is shown along with the power curve obtained from the voltages and the corresponding currents.

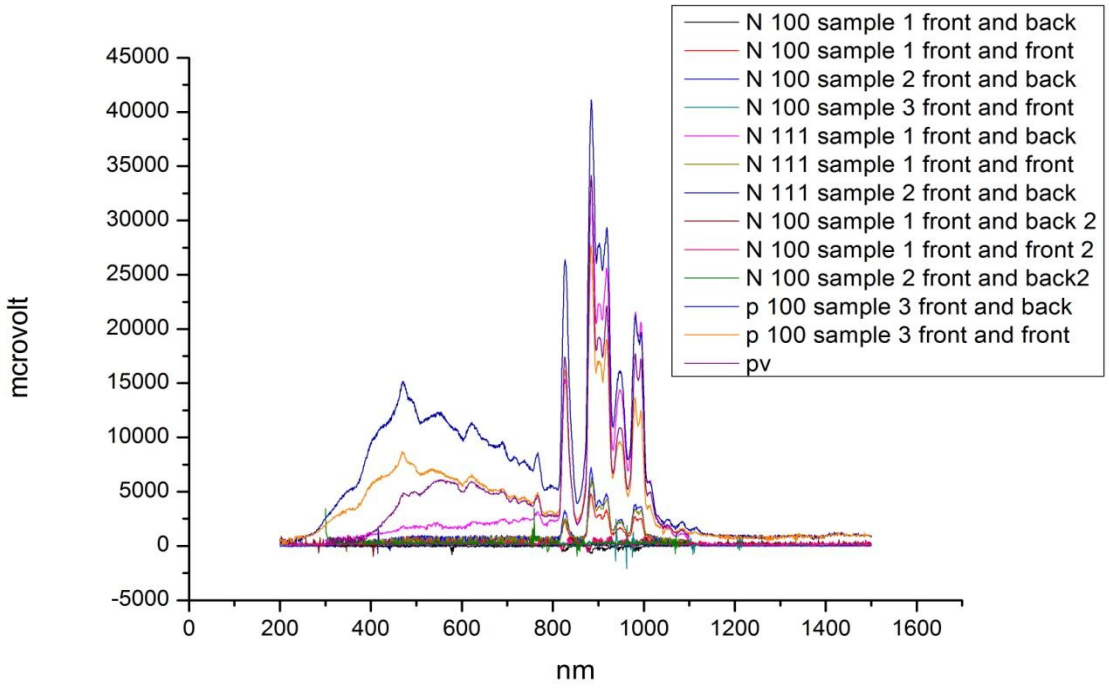


Figure 5.4 photovoltaic measurement of all the prepared samples

The maximum point of the power curve determines the point of maximum current (i.e Imax) and point of maximum voltage (i.e Vmax) from which the efficiency can be calculated. The light source use has the illumination power on the sample as follows:

Power of the lamp=(120x0.7) W = 84 watt
Distance to the sample=23cm

The source will be considered as a point source so that the distance from the source to the sample to be the radius, any point from the source should be considered as a sphere; therefore the area is given by:

Area = $4\pi r^2 = 4 \times \pi \times (23)^2 = 6647{,}6\ cm^2$

Now the input power to the solar surface (Pin) = $(light\ power)/area$

Pin = $84/6647.6\ W/cm^2$

Pin = $0.012636\ W/cm^2 = 12.636\ mW/cm^2$

Table 5.1 current, voltage and power of the multilayer porous silicon obtained from the method in 4.6.

| Current (A) | Voltage (V) | power(w) |
|---|---|---|
| 0,0158 | 0,0000 | 0,0000 |
| 0,0158 | 0,0280 | 0,0004 |
| 0,0155 | 0,0730 | 0,0011 |
| 0,0152 | 0,1500 | 0,0023 |
| 0,0149 | 0,1720 | 0,0026 |
| 0,0146 | 0,1820 | 0,0027 |
| 0,0143 | 0,1910 | 0,0027 |
| 0,0140 | 0,1960 | 0,0027 |
| 0,0137 | 0,2030 | 0,0028 |
| 0,0134 | 0,2080 | 0,0028 |
| 0,0131 | 0,2120 | 0,0028 |
| 0,0128 | 0,2160 | 0,0028 |
| 0,0125 | 0,2200 | 0,0028 |
| 0,0122 | 0,2230 | 0,0027 |
| 0,0119 | 0,2260 | 0,0027 |
| 0,0116 | 0,2290 | 0,0027 |
| 0,0113 | 0,2320 | 0,0026 |
| 0,0110 | 0,2350 | 0,0026 |
| 0,0107 | 0,2360 | 0,0025 |
| 0,0104 | 0,2390 | 0,0025 |
| 0,0000 | 0,2780 | 0,0000 |

So far we have seen that the maximum current and maximum voltage are obtained from the maximum point of power, therefore these are obtained from fig 5.4 as;

$I_{max}$ =13.4 mA/cm²

$V_{max}$ = 208 mV

Therefore, the efficiency is given by;

$\eta_g^p = I_{max} V_{max}/P_{in}$,

where $\eta^p$= efficiency of the porous sample prepared.

$\eta^p = (13.4 \times 208 \times 10^6)/(12.636 \times 10^3)$

$\eta^p = 0.2206$

$\eta^p = 22.06\ \%$

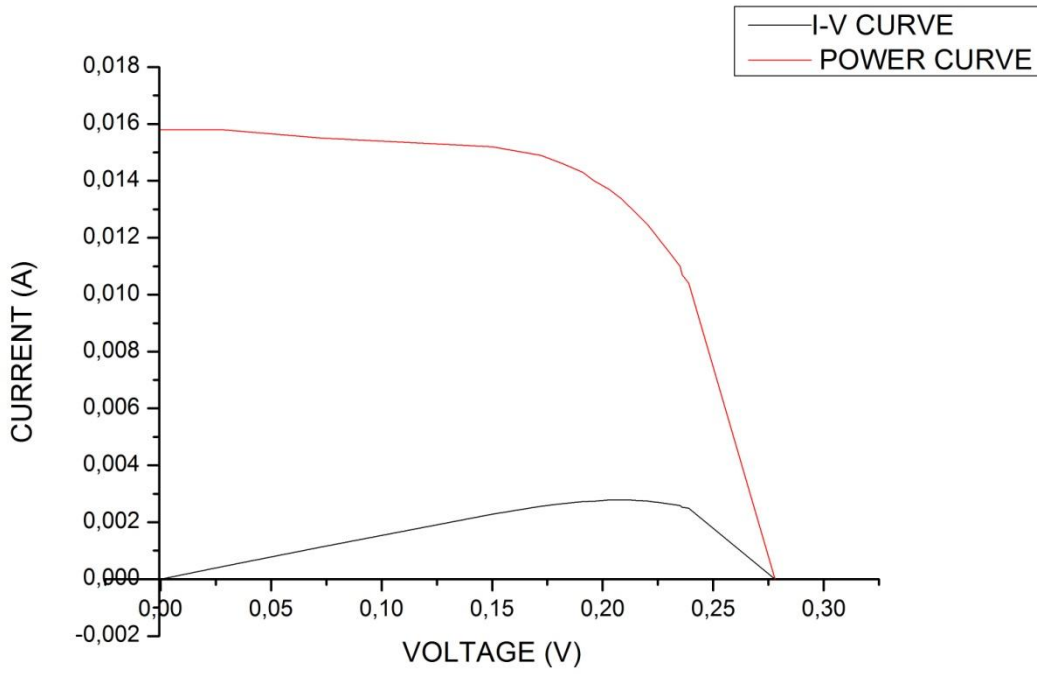


Figure 5.4 I-V curve and power curve on same graph, with 'B' equals to current in amperes/centimeter squares and 'A' equals to voltage in volts.

Now consider the non etched c-silicon from which the above mention porous silicon is made and the efficiency found to be 22.06%, the I-V values are obtained using same method as the one used above(i.e I-V measurement). The values where obtained as in table 5.2. The values shows corresponding low voltage and low current compared

to the prepared sample, which result in lower power and low efficiency as we can see below:

Already we know the power of our illumination as obtained above, now we can see that the maximum voltage (Vmax) and maximum current (Imax) that are corresponded with the maximum value of the power, we have:

Imax= 2.672mA/cm² and V=60.4090mV, and our Pin= 12.636mV/cm²
Therefore, the efficiency is;

$\eta_{\eta}$= (2.672x60.4090x$10^6$)/(12.636x$10^3$), where $\eta_{\eta}$= efficiency of the crystal silicon from which the sample is prepared(i.e non etched)

$\eta_{\eta}$=0.01277

$\eta_{\eta}$=1.277%

Table 5.2 current, voltage and power of the single layer porous silicon obtained from the method in 4.12

| current(mA/cm²) | Voltage (mV) | Power(mW) |
|---|---|---|
| 3.150 | 0 | 0 |
| 3,1500 | 16,7090 | 52,6334 |
| 3,0900 | 43,5650 | 134,6159 |
| 2,9710 | 49,9540 | 148,4133 |
| 2,9110 | 52,8580 | 153,8696 |
| 2,8510 | 55,4720 | 158,1507 |
| 2,7920 | 56,9240 | 158,9318 |
| 2,7320 | 58,9570 | 161,0705 |
| 2,6720 | 60,4090 | 161,4128 |
| 2,6120 | 61,5710 | 160,8235 |
| 2,5520 | 62,7330 | 160,0946 |
| 2,4930 | 63,8950 | 159,2902 |
| 2,4330 | 64,7660 | 157,5757 |
| 2,3730 | 65,6370 | 155,7566 |
| 2,3130 | 65,9000 | 152,4267 |
| 2,2540 | 66,7630 | 150,4838 |
| 2,1940 | 67,6260 | 148,3714 |
| 2,1340 | 67,9140 | 144,9285 |
| 2,0740 | 68,7770 | 142,6435 |
| 0,0000 | 80,0000 | 0,0000 |

If we compare the two efficiencies, it is clear that the multi-layer porous sample has higher efficiency than the crystalline silicon. Therefore we can see the enhancement by taking the differences between the two results which is;

$\eta_i$= increase in efficiency by the method observed in this thesis,

$\eta_i = (\eta_c^p - \eta_c^n)\%$

$\eta_i$ =(22.06-1.277)%=20.783%,

We can see from Fig 5.3, the I-V curves varies for the single layer porous and the multilayer with later have higher I-V curve indicating more efficiency compared with the former. More information can be obtained from the figure that shows the effect of the methods used on the c-silicon to enhance its efficiency. All the measurement were taken under same condition so that to realize the effect of what have been done to the wafer in order to manipulate the efficiency.

Throughout the study, some steps where repeated more than ones in order to get good result.

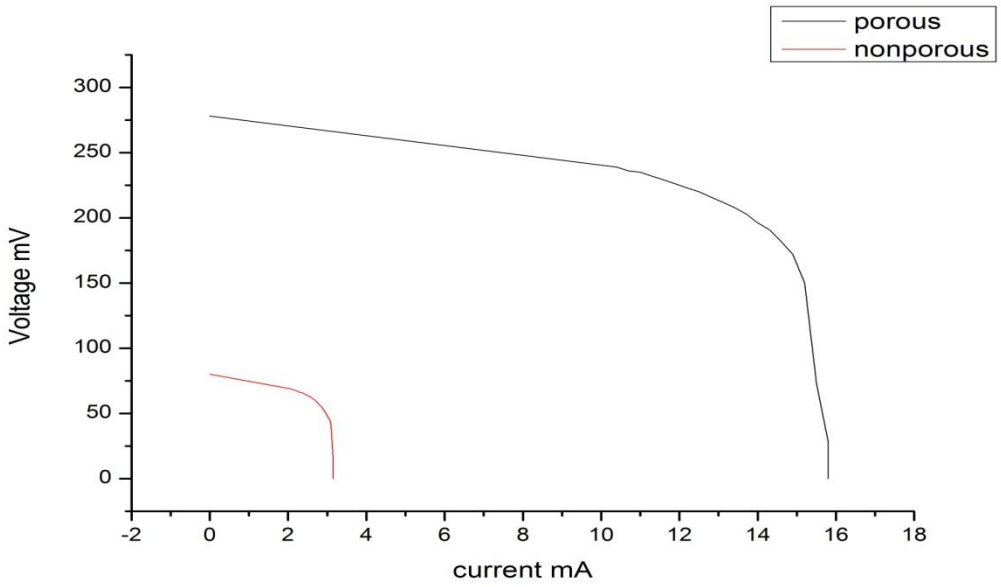


Figure 5.5 I-V curve of multilayer porous and single porous in comparison

# CHAPTER 6

# CONCLUSION

## 6.1 CONCLUSION

The thesis observed the effect of multilayered porous silicon toward enhancing quantum efficiency of the silicon solar cells. Quantum efficiency of the existing solar cells silicon based faced a lot of challenges such as reflecting most of the solar spectrum. Therefore the photon/electron conversion will be less only those portion of the spectrum can be processed for the conversion.

The steps taken were the etching of the P-type porous silicon using anodizationtion technique. And then the production of nanoporous, which further doped with N-impurities and formed P-N Junction. These nanoporous, were not completely doped because of the heterojunction that formed between the crystal and the etched portion of the device. Moreover, the surface became rough.

Going by the discussion, it shows that by taking the previous steps mention in chapter three of this thesis the quantum efficiency of crystalline silicon was enhanced by approximately 20.783% which is significant in solar application. Moreover, the doping or amount of impurity in the crystalline silicon also is important. If we apply same method on high efficient wafer (i.e the low resistive wafer) we can obtain higher efficiency through enhancing by 20.783% of its original value.

Furthermore, more absorption of solar spectrum can be observed using same method. These can be used in many applications that needs higher absorption of the spectrum.In comparism, the fabricated solar, show an increase in the solar spectrum at the UV and IR part of the spectrum as shown in fig 5.3.

At last but not the least, the net quantum efficiency may be further enhanced by adjusting some of the steps used in this study.

# REFERENCES


[1] Canham, L.C, "Properties of porous silicon" Malvern, UK, September 1997.

[2] Elisabet Xifré Pérez "Fundementals of porous silicon", Universitat Rovira,U.R.I.V T.2181-2007

[3] E. Lorenzo, C.J. Oton, N.E. Capuj, M. Ghulinyan, D. Navarro Urrios, Z. Gaburro, and L. Pavesi, "Applied Optics", Vol., 44, pp 5415 2005.

[4] U. Gaining, A. Yelon "Thin Solid Films" vol.255 p. 135 Switzerland 1995

[5] U. Gaining, A. Yelon ;"Diplomarbeit Physik" T.U. Munchen, Germany, 1994

[6] G. Amato, V. Bullara, N. Brunetto, L. Boarino "Thin Solid Films" vol.276 p.204 (Switzerland) 1996

[7] G. Amato, V. Bullara, N. Brunetto, L. Boarino "Mater. Lett." vol.26 p.295 Netherlands 1996

[8] Dorothy M.Hoffman, JohnH.Thomas, and BawaSingh "High vacuum science and technology" elsevier science and technology books, October 1997

[9] Manijeh Razeghi Walter P. Murphy "Technology of Quantum Devices" p27-37 Springer New York Dordrecht Heidelberg London, 2009

[10] D. Briggs , "Handbook of X-ray and ultraviolet photoelectron spectroscopy" pp.398 Heyden1977

[11] M. Orhring, "The Materials Science of Thin Films", Academic Press, 1992

[12] Guozhong Cao ,"Nanostructures & Nanomaterials" , İmperial College Press , 2004

[13] Denis Semwogerere, Eric R. Weeks , "Encyclopedia of Biomaterials and Biomedical Engineering" , Taylor & Francis, 2005

[14] LT. Canham, A.G. Cullis, C. Pickering, O.D. Dosser, T.I. Cox, T.P. Lynch "Nature" vol.368 p. 133 (UK) 1994

[15] U. Gaining, A. Yelon “Thin Solid Films” vol.255 p. 135 Switzerland 1995.

[16] U. Gaining, A. Yelon ‘Diplomarbeit Physik’, T.U. Munchen, Germany, 1994

[17] O. Belmont, D. Bellet, Y. Brechet “ J. Appl Phys” vol.79 p.7586 USA 1996.

[18] St. Frohnhoff, R. Arens-Fischer, T. Heinrich, J. Fricke, M. Arntzen, W. Theiss “Thin Solid Films” vol.255 p.ll5 Switzerland 1995.

[19] J. Von Behren, P.M. Fauchet, E.H. Chimowitz, CT. Lira “Mater. Res. Soc. Symp. Proc.” vol.452 p.565 USA 1997.

[20] G. Amato, V. Bullara, N. Brunetto, L. Boarino “Thin Solid Films” vol.276 p.204 Switzerland 1996.

[21] G. Amato, N. Brunetto “Mater. Lett.” vol.26 p.295 Netherlands 1996.

[22] P.L. Ossicini S. L. and Priolo F, Light emitting silicon for microphotonics, Springer-Verlag, Berlin Heidelberg 2003.

[23] Michael J Morgan, Greg Jakovidis and Ian McLeod ‘An experiment to measure the I-Vcharacteristics of a siliconnsolar cell’ Department of Physics, Monash University, Clayton, Victoria 3168, Australia

[24] Thomas J. Fellers and Michael W. Davidson and Kenneth R. Spring ‘molecular expression ptical microscopy prime physics of light and color ‘- Scientific Consultant, Lusby, Maryland, 20657. - National High Magnetic Field Laboratory, 1800 East Paul Dirac Dr., The Florida State University, Tallahassee, Florida, 32310.

[25] MBE Laboratory in the Institute of physics of the ASCR IOP ASCR, Division solid state physics, praha 6, cukrovarnicka 10, mbe@fzu.com

[26] J. Rouquerol et al ‘Pure Appl. Chem’. vol.66 no.8 p. 1739-58 UK 1994.

[27] G. Mauckner et al “ J. Lumin” vol.57 p.211-5 Netherlands 1993.

[28] D. Brumhead, LT. Canham, DM. Seekings, PJ. Tufton “Electrochim Acta” vol.38 no.2/3 p.l91-7 UK 1993.

[29] M. Enachescu, E. Hartmann, F. Koch “ J. Vac. Sci. Technol. B” vol.12 no.3 p.2074-7 USA 1994.

[30] Th. Dittrich et al “Appl. Phys. Lett” vol.67 p.l 134-6 USA 1995.

[31] TR. Guilinger, MJ. Kelly, EH. Chason, TJ. Headley, AJ. Howard " J. Electrochem. Soc" vol.142 p. 1634 1995.

[32] Th. Dittrich, I. Sieber, S. Rauscher, J. Rappich "Thin Solid Films" vol.226 p.200-3 Switzerland 1996.

[33] S.L. Yau et al "J. Electrochem. Soc." vol.141 no.2 p.402-9 USA 1994.

[34] FB. Dudel, MM. Pieger, JP. Pickering, JL. GoIe, PA. Kohl, LA. Bottomly " J. Electrochem. Soc". vol.143 no.8 p.L164-6 USA 1996.

[35] J.L. GoIe, FB. Dudel, D. Grantier, DA. Dixon "Phys. Rev. B" vol.56 no.4 p.2137-53 USA 1997.

[36] T. Unagami, M. Seki "J. Electrochem. Soc". vol. 125 no.8 P 1339-44USA 1978.

[37] H. Baumgart, R.C. Frye, L.E. Trimble, HJ. Leamy, G.K. Celler in "Laser and Electron Beam Interactions With Solids" p.609-14 Elsevier, 1982.

[38] V. Labunov, V. Bondarenko, L. Glinenko, A. Dorofeev, L. Tabulina "Thin Solid Films" vol.137 p. 123-34 Switzerland 1986.

[38] P.C. Searson "Appl. Phys. Lett". vol.59 p.832-4 USA 1991.

[39] D.R. Turner " J. Electrochem. Soc". vol. 105 no.7 p.402-8 USA 1958.

[40] I. Sagnes, A. Halimaoui, G. Vincent, PA. Badoz "Appl. Phys. Lett." vol.62 p.1155-7 USA 1993.

[41] Y. Kanemitsu, H. Uto, Y. Masumoto, T. Matsumoto, T. Futagi, H. Minivra "Phys. Rev. B" vol.48 no.4 p.2827 USA 1993.

[42] N. Ookubo, Y. Matsuda, Y. Ochai, N. Kuroda "Mater. Sci. Eng. B" vol.20 no.3 p.324-7 Switzerland 1993.

[43] P. MaIy, F. Trojanek, A. Hospodkova, V. Kohlova, I. Pelant "Solid State Commun." vol.89 no.8 p.709 USA 1994.

[44] X. Xie et al "Phys. Rev. B" vol.49 no.8 p.5386-97 USA 1994.

[45] ZC. Feng, A.T.S. Wee, K.L. Tan "J. Phys. D" vol.27 p.1968 UK 1994.

[46] R. Laiho, A. Pavlov "Phys. Rev. B" vol.51 p.R14774 USA 1995.

[47] S. Guha, G. Hendershot, D. Peebles, P. Steiner, F. Kozlowski, W. Lang "Appl. Phys. Lett." vol.64 no.5 p.613 USA 1994.

[48] J.L. Heinrich, CL. Curtis, G.M. Credo, K.L. Kavenagh, MJ. Sailor "Science" vol.255 p.66-8USA 1992.

[49] Y. Watanabe, Y. Arita, T. Yokoyama, Y. Igarashi "J Electrochem. Soc." vol.122 p.1351 USA 1975.

[50] T. Unagami "J. Electrochem. Soc" vol. 127 no.2 p.476-83 USA 1980.

[51] R. Herino, G. Bomchil, K. Barla, C. Bertrand, J.L. Ginoux "J. Electrochem. Soc." vol.134 no.8 p.1994-2000 USA 1987.

[52] LL. Baranov, VP. Bondarenko, A.M. Dorofeev, LV. Tabulina "Vestsi Akad. Navuk BSSR, Ser. Khim Navuk" vol.6 p.36-9 Byelorussia 1988.

[53] X.G. Zhang "J. Electrochem. Soc." vol. 138 no. 12 p.3750-6 USA 1991.

[54] H. Unno, K. Imai, S. Muramoto "J Electrochem. Soc." vol.134 p.645 USA 1987.

[55] P.H. Bellin, W.K. Zwicker " J. Appl. Phys". vol.42 no.3 p. 1216-21 USA 1971.

[56] R.L. Meek "J. Electrochem. Soc." vol. 118 no.3 p.437-42 USA 1971.

[57] MJ. Hill "J. Electrochem. Soc." vol.120 no.l p.142-5 USA 1973.

[58] J. Harsanyi, HU. Habermeier "Microelectron. Eng." vol.6 p 85 Netherlands1987

[59] O. Bisi, S. Ossicini, and L. Pavesi, "Surf. Sci. Rep"., **38**, 1 2000.

[60] K. D. Hirschman, L. Tsybeskov, S. P. Duttagupta, and P. M. Fauchet, "Nature," **384**, 338 1996.

[61] C. C. Striemer and P. M. Fauchet, "Appl. Phys. Lett.", **81**, 2980 2002.

[62] C. Mazzoleni and L. Pavesi. "Appl. Phys. Lett.", **67**, 2983 1995.

[63] V.S.Y. Lin, K. Motesharei, K.P.S. Dancil, M.J. Sailor, M.R. Ghadiri, "Science", **278**, 840 1997.

[64] S. Chan, P.M. Fauchet, Y. Li, L.J. Rothberg, and B.L. Miller, "Phys. Stat. Solidi A," **182**, 541 2000.

[65] F. Cunin, T.A. Schmedake, J.R. Link, Y.Y. Li, J. Koh, S.N. Bhatia, M.J. Sailor, “Nature Mater.”, **1**, 39 2002.

[66] W. Theiss, “Surf. Sci. Rep.”, **29**, 91 1997.

[67] D.R. Turner,” J. Electrochem. Soc.”, **138**, 807 1991.

[68] R.L. Smith, and S.D. Collins,” J. Appl. Phys”. **71**, R1 1992.

[69] A. J. Bard, “Encyclopedia of Electrochemistry of the Elements,” Dekker, New York 1986.

[70] A.K. Vijh,” Electrochemistv of Metals and Semiconductors”, Dekker, New York 1973.

[71] B.E. Conway, J.O’M. Bockris, E. Yeager, S.U.M. Khan, and R.E. White, “Comprehensive Treatise of Electrochemistry” Vol. 7, Plenum, New York, 1983.

[72] P. J. Holmes, “The Electrochemistry of Semiconductors”, Academic, London, 1962.

[73] E. A. Efimov and I. G. Erusalimchik, “Electrochemistry of Germanium and Silicon”, Sigma, London 1963.

[74] J.B. Flynn, “J. Electrochem. Soc.”, **105**, 715 1958.

[75] H. Foll, “Appl. Phys. A”, **53**, 8 1991.

[76] L. Canham, New Scientist, **1868** 1993.

[77] M.I.J. Beale, J.D. Benjamin, M.J. Uren, N.G. Chew, and A.G. Cullis, “J. Cryst. Growth,” **73**, 622 1985.

[78] L. Pavesi,” J. Appl. Phys.” **80**, 216 1996.

[79] T. Trifonov, A. Rodriguez, F. Servera, L.F. Marsal, J. Pallarès, R. Alcubilla, “phys. stat. sol.” (a), **202**, 1634 2005.

[80] P. Müller, IUPAC Manual of Symbols and Technology, "Pure Appl. Chem.", **31**, 578 1972.

[81] A. Bruyant, G. Lérondel, P.J. Reece, and M. Gal." Appl. Phys. Lett". **82**, 3227 2003.

[82] H. S. Nalwa, Silicon Based Materials and Devices, Vol. 2: "Properties and Devices," Academic Press, San Diego 2001.

[83] J. Charrier, M. Guendouz, L. Haji, and P. Joubert, "Phys. Stat. Sol" (a), **182**, 431 2000.

[84] L. De Stefano, L. Moretti, A.M. Rossi, and I. Rendina, "Sen. Actuators A", **104**, 179 2003.

[85] J. Volk, J. Balázs, A.L. Tóth, and I. Bársony, "Sen. Actuators B", **100**, 163 2004.

[86] E.K. Squire, P.A. Snow, P.St. Russell, L.T. Canham, A.J. Simons, and C.L. Reeves, "J. Luminescence," **80**, 125 1999.

[87] A. Halimaoui, "Porous Silicon formation by anodization" (in Properties of Porous Silicon), L. Canham, Ed., Short Run Press Ltd., London 1997.

[88] C. Mazzoleni, "Tesi di Laurea," Universitá di Trento 1995.

[89] L. Pavesi, and V. Mulloni, "J. Luminescence," **80**, 43 1999.

[90] E. Lorenzo, C.J. Oton, N.E. Capuj, M. Ghulinyan, D. Navarro Urrios, Z.